Journal of Applied Fluid Mechanics, Vol. 12, No. 1, pp. 303-309, 2019.
Available online at www.jafmonline.net, ISSN 1735-3572, EISSN 1735-3645.
DOI: 10.29252/jafm.75.253.29091

CFD Analysis of Aerodynamic Drag Effects on Vacuum Tube Trains

S. A. Gillani[1], V. P. Panikulam[1], S. Sadasivan[1†] and Z. Yaoping [2]

[1]*School of Mechanical Engineering, Vellore Institute of Technology, India-632 014*
[2]*Evacuated Tube Transport, Southwest Jiaotong University, Chengdu 610031, China.*

†*Corresponding Author Email: sreejas66@gmail.com*

(Received April 10, 2018; accepted September 3, 2018)

ABSTRACT

Aerodynamic aspects of train shapes suitable for Vacuum Tube Train System are investigated in this paper. Three feasible geometries for the vacuum tube train system have been considered and modelled in three dimensions and have been computationally studied using the commercial software Ansys Fluent. Aerodynamic drag loads on these geometries have been calculated under different tube pressures and speeds of the train, which provide insight on various operating parameters that need to be considered while designing the vacuum tube train system. The present computational research shows that, the suitable vacuum pressure, and different shapes of head and tail of the train have significantly effects the drag force of the vacuum train in the tunnel. Overall, the elliptical train shape with a height to base ratio of 2:1 is more efficient for aerodynamic drag reduction of the vacuum tube train at the vacuum tube pressure of 1013.25 Pa.

Keywords: CFD; Aerodynamic drag; Vacuum train; Shock wave; Navier stokes equations.

NOMENCLATURE

e	Internal energy per unit mass	ρ	density of gas
k	turbulence kinetic energy	τ	viscous stress
p	gas Pressure	λ	bulk viscosity coefficient
u, v, w	velocity components in x, y and z directions respectively	μ	molecular viscosity coefficient
V	absolute velocity	ε	rate of dissipation

1. INTRODUCTION

Trains are locomotives used to carry cargo or passengers from one destination to another. The conventional mode of transportation is expensive or relatively slow or a combination of both. Until recently, trains have been limited to maximum speeds of 300-350 kmph. But, in the current generation, where everything is moving fast, there is a need for reaching destinations faster, so that time is not wasted on travel. This has led to the formulation of new high speed transportation networks such as Vacuum Tube Trains. Though, still at the conceptualization stage, scientists have made huge progress in this field. Vacuum Tube Trains, theoretically speaking, can reach speeds of up to 1000 km/h, Zhang (2012). This will hence be the future of ground transportation. The vacuum tube train system needs to take into consideration many more parameters in comparison to the conventional trains. Kim *et al*. (2011) and Zhang *et al*. (2011) shows that the aerodynamic drag, development of shocks and maintenance of low pressures in the tube are the major drawbacks which need to be controlled in order to get a successful transportation system. Hence there is a requirement to study the aerodynamic drag acting on these bodies in order to find out the suitable ranges of pressure to be maintained in the tunnel, velocity that the trains can run and the suitable geometry for the trains, Zhi-yun *et al*. (2005) and Chen *et al*. (2012). Kwon *et al*. (2001) have showed that the vacuum tube trains need to run at low pressure in order to achieve the high speed. But maintaining the tunnel at extremely low pressures is an insurmountable task and hence an achievable level of pressure to be maintained in the tunnel needs to be identified. The speed at which the trains run cannot exceed a certain level as this would result in shocks which would destroy the train system. Hence, a suitable speed with which

the train can run without the formation of uncontrolled shocks need to be identified as well. The geometry of the train is another parameter that is crucial to the modelling of the vacuum tube train system. Different geometries of trains have been identified and modelled. Bibin *et al.* (2013) found that a blockage ratio of 0.25 would be most appropriate for vacuum tube transportation. This effect taking into consideration with the assumption that the flow is steady three dimensional, compressible. The Navier-Stokes equations coupled with k-epsilon turbulent modelling were solved to calculate the aerodynamic drag acting on the train.

2. METHODOLOGY

2.1 Equations Of Fluid Motion

The compressible flow Navier Stokes Equations coupled with the k-ε equations for turbulent modelling have been solved using the Fluent software. The following assumptions have been considered during the process:

- Steady flow
- Compressible flow
- Three dimensional, turbulent flow
- Flow similar to that of a calorically perfect gas

The various governing equations which have been used in the analysis are as follows:

Continuity Equation:

$$\frac{\partial \rho}{\partial t}+\nabla.(\rho \vec{V})=0 \cdots\cdots\cdots\cdots \quad \ldots(1)$$

Momentum Equation:

X-Momentum

$$\frac{\partial(\rho u)}{\partial t}+\frac{\partial(\rho u^2)}{\partial x}+\frac{\partial(\rho uv)}{\partial y}+\frac{\partial(\rho uw)}{\partial z}=$$
$$-\frac{\partial p}{\partial x}+\frac{\partial}{\partial x}\left(\left(\lambda\nabla\cdot\vec{V}\right)+2\mu\frac{\partial u}{\partial x}\right)+\frac{\partial}{\partial y}\left[\mu\left(\frac{\partial v}{\partial x}+\frac{\partial u}{\partial y}\right)\right]$$
$$+\frac{\partial}{\partial z}\left[\mu\left(\frac{\partial u}{\partial z}+\frac{\partial w}{\partial x}\right)\right]\ldots\ldots\ldots\ldots\ldots \quad \ldots\ldots(2)$$

Y-Momentum

$$\frac{\partial(\rho v)}{\partial t}+\frac{\partial(\rho uv)}{\partial x}+\frac{\partial(\rho v^2)}{\partial y}+\frac{\partial(\rho vw)}{\partial z}=$$
$$-\frac{\partial p}{\partial y}+\frac{\partial}{\partial x}\left[\mu\left(\frac{\partial v}{\partial x}+\frac{\partial u}{\partial y}\right)\right]+\frac{\partial}{\partial y}\left(\left(\lambda\nabla\cdot\vec{V}\right)+2\mu\frac{\partial v}{\partial y}\right)$$
$$+\frac{\partial}{\partial z}\left[\mu\left(\frac{\partial w}{\partial y}+\frac{\partial v}{\partial z}\right)\right]\ldots\ldots\ldots\ldots\ldots \quad \ldots\ldots(3)$$

Z-Momentum

$$\frac{\partial(\rho w)}{\partial t}+\frac{\partial(\rho uw)}{\partial x}+\frac{\partial(\rho vw)}{\partial y}+\frac{\partial(\rho w^2)}{\partial z}=$$
$$-\frac{\partial p}{\partial z}+\frac{\partial}{\partial x}\left[\mu\left(\frac{\partial u}{\partial z}+\frac{\partial w}{\partial x}\right)\right]+\frac{\partial}{\partial y}\left[\mu\left(\frac{\partial w}{\partial y}+\frac{\partial v}{\partial z}\right)\right]$$
$$+\frac{\partial}{\partial z}\left(\left(\lambda\nabla\cdot\vec{V}\right)+2\mu\frac{\partial w}{\partial z}\right)\ldots\ldots\ldots\ldots \quad \ldots\ldots(4)$$

Energy Equation

$$\frac{\partial}{\partial t}\left[\rho\left(e+\frac{V^2}{2}\right)\right]+\nabla\cdot\left[\rho\left(e+\frac{V^2}{2}\vec{V}\right)\right]=$$
$$\rho\dot{q}+\frac{\partial}{\partial x}\left(k\frac{\partial T}{\partial x}\right)+\frac{\partial}{\partial y}\left(k\frac{\partial T}{\partial y}\right)+\frac{\partial}{\partial z}\left(k\frac{\partial T}{\partial z}\right)$$
$$-\frac{\partial(up)}{\partial x}-\frac{\partial(vp)}{\partial y}-\frac{\partial(wp)}{\partial z}$$
$$+\frac{\partial(u\tau_{xx})}{\partial x}+\frac{\partial(u\tau_{yx})}{\partial y}+\frac{\partial(u\tau_{zx})}{\partial z}$$
$$+\frac{\partial(v\tau_{xy})}{\partial x}+\frac{\partial(v\tau_{yy})}{\partial y}+\frac{\partial(v\tau_{zy})}{\partial z}$$
$$+\frac{\partial(w\tau_{xz})}{\partial x}+\frac{\partial(w\tau_{yz})}{\partial y}+\frac{\partial(w\tau_{zz})}{\partial z}\ldots\ldots\ldots\ldots \quad \ldots\ldots(5)$$

k Equation:

$$\frac{\partial}{\partial t}(\rho k)+\frac{\partial}{\partial x_i}(\rho k u_i)=\frac{\partial}{\partial x_j}\left[\left(\mu+\frac{\mu_t}{\sigma_k}\right)\frac{\partial k}{\partial x_j}\right]$$
$$+G_k+G_b-\rho\varepsilon-Y_M+S_k\ldots\ldots\ldots\ldots\ldots\ldots\ldots\ldots(6)$$

ε EQUATION:

$$\frac{\partial}{\partial t}(\rho\varepsilon)+\frac{\partial}{\partial x_i}(\rho\varepsilon u_i)=\frac{\partial}{\partial x_j}\left[\left(\mu+\frac{\mu_t}{\sigma_\varepsilon}\right)\frac{\partial \varepsilon}{\partial x_j}\right]$$
$$+C_{1\varepsilon}\frac{\varepsilon}{k}\left(G_k+C_{3\varepsilon}G_b\right)-C_{2\varepsilon}\rho\frac{\varepsilon^2}{k}+S_\varepsilon\ldots\ldots\ldots(7)$$

2.2 Details of Vacuum Tube Train System

The schematic representation of vacuum tube train system considered in the present study is shown in Fig. 1. The various dimensions of the vacuum tube train system are as follows:

- Train Diameter = 2 m
- Train Length = 40 m
- Tunnel Diameter = 3.2 m
- Tunnel Length = 200 m
- Blockage Ratio = 0.4

The train shape has been assumed as an axisymmetric body. Additionally the flow induced by the train motion has been taken as three dimensional in nature. The simulations have been carried out to replicate the wind tunnel test of a three dimensional train shape. Thus the body has been taken as stationary and the inlet of the

computational domain has been set with velocity corresponding to train speed and tunnel ambient pressure. The outer surfaces of the train were treated as no slip walls. Pressure outlet condition has been set for the outlet of the computational domain. The tunnel inner surface has been considered as a wall moving in x direction.

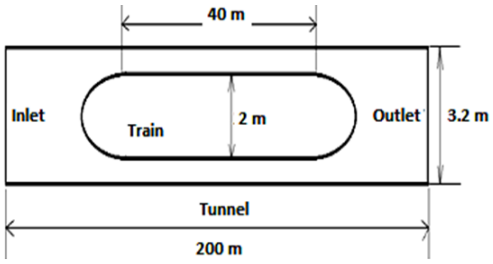

Fig. 1a. Vacuum Tube Train System.

2.3 Geometry and Mesh Details

The meshing of the vacuum tube train system has been carried out using ICEM CFD Software. The entire computational domain has been meshed using hexahedral mesh and at the inlet and outlet of the train O-Grid has been used in order to develop even finer meshes as these locations are sensitive to high fluctuations of shocks. This also provides proper meshing at these curved entities as the meshing might not be evenly placed along the curve. The meshed model (surface mesh) of the optimized train model is portrayed in Fig. 2a and that of slice mesh in Fig. 2b.

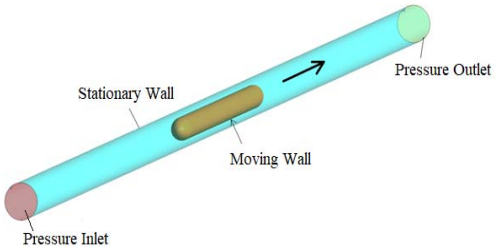

Fig. 1b. Boundary conditions in the computational domain.

Fig. 2a. Meshing of the vacuum tube train system.

Fig. 2b. Slice mesh of the vacuum tube train system.

2.4 Boundary Conditions

The various parts of the vacuum tube train system have been shown in Fig. 1 and the different boundary conditions specified in computational domain of the current simulations are also shown in Fig. 2. The pressure has been varied between 101325, 10132.5, 1013.25 and 101.325 Pa and each time the simulations have been performed. Similarly, the Mach number has been varied based on the desired speed of the train and each time the simulations have been performed. The different Mach numbers used are 0.72, 0.792, 0.864, 0.936 and 1.008. The various boundary conditions used are as follows:

Inlet: Pressure inlet with a pressure of 1013.25 Pa and at a Mach number of 0.936.

Train: Considered to be a wall moving in x direction.

Outlet: Exit of the tunnel is specified as pressure outlet.

Tunnel: Considered to be stationary wall with no slip condition.

3. Results And Discussion

In the present computational study, the main idea is to find suitable parameters mainly, operating vacuum pressure, speed of the train and the shape for the vacuum tube train system. This involves solving the equations mentioned earlier using the Fluent Software. Once the simulations have been carried out, the results have to be analysed in order to get the suitable parameters.

3.1 Comparison of Pressure

In this stage, the elliptical train with a height to base ratio of 2:1 has been taken and using this geometry and keeping the velocity of the tunnel as 250 m/s, the simulations were carried out on different pressure levels to be maintained in the tunnel such as 101.325 Pa, 1013.25 Pa, 10132.5 Pa and 101325 Pa. The drag force values were computed and have been plotted with respect to the pressure values in Fig. 3. It is visible that as the pressure increases, the force also increases. It can also be noted that as pressure decreases beyond a certain point, the drop in force is negligible. Considering the cost and implementation ease factors, trying to maintain very low pressures within the entire length of the tunnel will be very expensive and it is very difficult to achieve. Hence, considering all these factors, it is safe to maintain tunnel ambient pressure almost 100 times lesser than the atmospheric pressure.

3.2 Comparison of Mach Number

The current trains run at maximum speeds of about 100 m/s. But the vacuum tube trains can run much faster than this but it is necessary to compute the suitable velocity with which these trains can travel as there are numerous drawbacks of running at high speeds. Hence in the next stage of the simulation and analysis, the suitable velocity with which the train can travel without much shocks and disturbances was determined, which in turn helped

Table 1 Drag force and drag coefficient corresponding to various velocities

Velocity (m/s)	Mach Number	Drag Force(N)	Drag Coefficient
250	0.72	3410	0.0927
275	0.792	4361	0.1039
300	0.864	4705	0.1202
325	0.936	4767	0.1297
350	1.008	5499	0.1429
375	1.081	5681	0.1546

in calculating the Mach number and Reynold's number. In this case too, the elliptical train geometry with a height to base ratio of 2:1 was considered for the simulations and the pressure maintained in the tunnel was 1013.25 Pa. Simulations were carried out for different velocities such as 250 m/s, 275 m/s, 300 m/s, 325 m/s, 350 m/s and 375 m/s and the force acting in each case has been tabulated in Table 1.

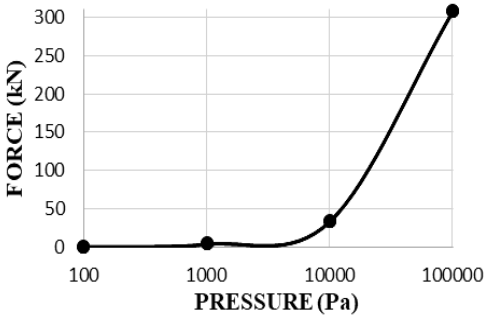

Fig. 3. Force acting at different pressure values with a velocity of 250 m/s and a blockage ratio of 0.4.

The Reynold's number was calculated for the individual velocities and these values of Reynold's number were plotted with respect to the drag force and this graph is shown in Fig. 4.

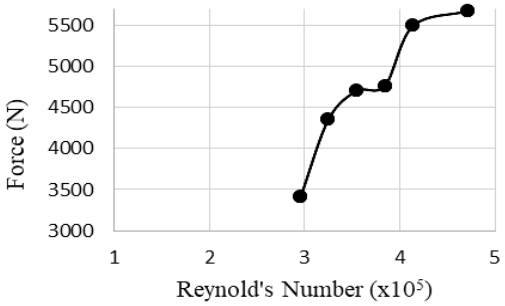

Fig. 4. Force acting corresponding to different velocities 4.2.

It can be noted that the force increases gradually until a Reynold's number of 384299 after which the force value shoots up. This value of Reynold's number corresponds to a Mach number of 0.936 and a velocity of 325 m/s. Mach numbers ranging from 0.8 to 1.0 corresponds to the transonic range. When the train runs at such speeds normal shocks will be formed which affect the stability of the train. On increasing the Mach number further, it reaches the supersonic region. If the trains were to run in supersonic conditions, more shocks would be produced and it will be very difficult to stabilize the train. The subsonic range which is between Mach number 0.3 and 0.8 is better as there would not be any shocks created but the aim of the vacuum tube train is to achieve very high speeds and that is not possible if the train runs in the subsonic range. The Mach contours corresponding to different velocities are shown in Figs. 4(a-f). The Mach number contours clearly show the supersonic nature of the flow downstream of the train body. This can be attributed to the flow path variation resulting from the presence of train shape inside the constant area tunnel. As the train speed increases the shock structure downstream of the train become more complex. Such strong shock interactions on the tunnel wall can rupture the tunnel in long run. Moreover, this situation may elevate the difficulty level in preparing the tunnel for another run. One possible solution to avoid such complex shock structure, while maintaining high train speed is heating of the tunnel. However, the economic feasibility and comfort level of this need to be addressed before proceeding with this proposal.

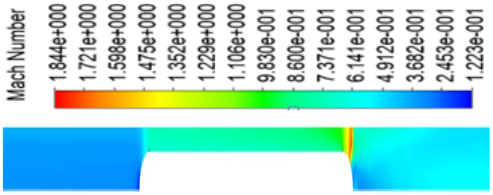

Fig. 4a. Mach contour corresponding to a velocity of 250 m/s.

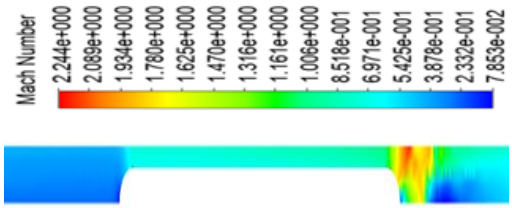

Fig. 4b. Mach contour corresponding to a velocity of 275 m/s.

The drag force experienced by the train needs to be assessed before choosing a particular train speed for real time run. The main drag contributor to the total drag on the train is pressure drag. Hence to understand the pressure variation over the train body at different train speeds, a surface pressure comparison is made in Fig. 4g. As it is clear from this figure, the maximum pressure is achieved at the front stagnation point of the train at all speeds. Moreover, the surface pressure values found to be increasing with train speed, especially at the front region of the train. The pressure at the head section of the train remain almost unaltered at all speeds. In Fig. 4c, the shock waves are existing at the rear side of the vacuum train and the oblique shock waves coexit with the normal shock waves that are developed by the continuous refection and interactions between the tunnel and the vacuum train walls. However, the strength of those interactions is comparatively less up to the velocity of train is 325 m/s. It is to be noted that the drastic increase in aerodynamic drag is generating when the Mach no exceed one or speed of accelerated flow field exceeds 325 m/s as in Table1. There is a considerable increase in surface pressure when velocity increased from 325 m/s to 350 m/s. This would be due to formation of shock waves. This inference is again well supported by the sudden rise in drag observed in Fig. 4g. After taking these aerodynamic aspects into consideration the suitable train velocity has been proposed as 325 m/s.

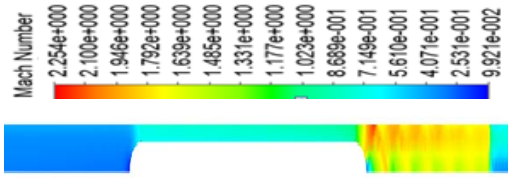

Fig. 4c. Mach contour corresponding to a velocity of 300 m/s.

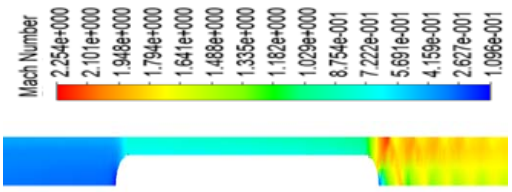

Fig. 4d. Mach contour corresponding to a velocity of 325 m/s.

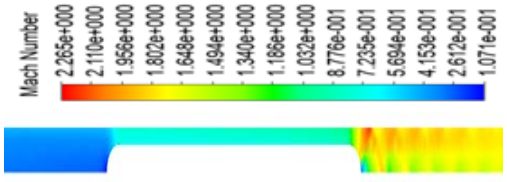

Fig. 4e. Mach contour corresponding to a velocity of 350 m/s.

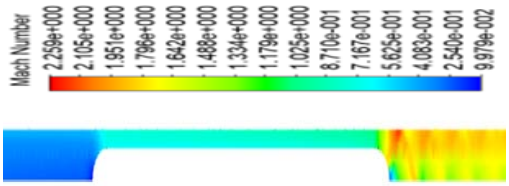

Fig. 4f. Mach contour corresponding to a velocity of 375 m/s.

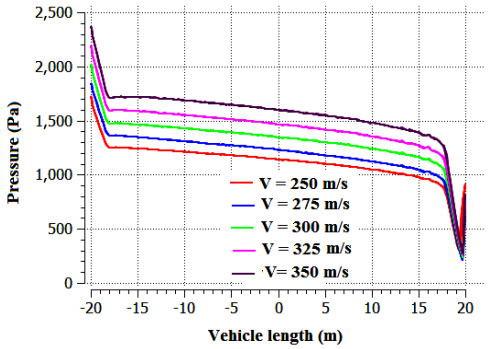

Fig. 4g. Pressure variation along the train for different velocity at 1013.25 Pa.

3.3 Simulation Of Train with Different Shapes

The next step is to decide on which geometry would be feasible for the train. There are three different geometries considered and they are shown in Figs. 5(a-c)

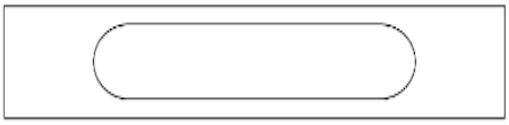

Fig. 5a. Elliptical head and tail with a height to base ratio of 1:1.

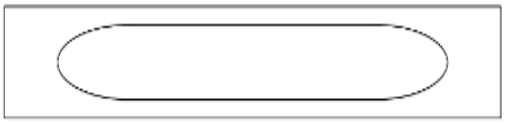

Fig. 5b. Elliptical head and tail with a height to base ratio of 2:1.

Fig. 5c. Triangular head and tail with a bottom to height ratio of 1:2.

In this stage, the simulations have been carried out with the suitable pressure of 1013.25 Pa, velocity of 325 m/s and Mach number of 0.936 on the three different geometries and their results are tabulated in Table 2.

Table 2 Force values corresponding to various geometries

GEOMETRY	FORCE (N)	VISCOUS COEFFICIENT
Semi circular (1:1)	5327	0.6784
Ellipse (2:1)	4767	0.1297
Triangle	4876	0.4431

From the Table 2 , it is noticed that among the three type of streamlined geometry ,the train with semicircular tail and head possess the maximum drag force, while the elliptical geometry with a height to base ratio of 2:1 has the lowest value of drag force. This result shows that, the aerodynamic drag of is highly affected by the head and tail shape of the train. The pressure contours of all the geometries are shown in Figs. 6(a-c).

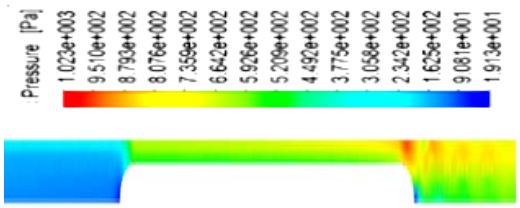

Fig. 6a. Pressure contour corresponding to the elliptical train with a height to base ratio of 2:1.

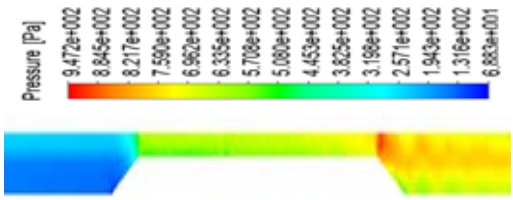

Fig. 6b. Pressure contour corresponding to the elliptical train with a height to base ratio of 1:1.

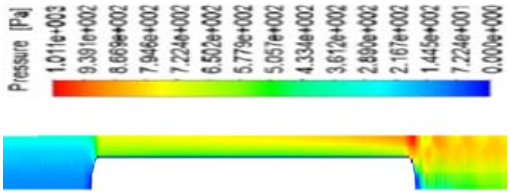

Fig. 6c – Pressure contour corresponding to the train with a triangular head and tail.

On analysis of the Mach and pressure contours, it can be seen that the elliptical geometry with a height to base ratio of 2:1 seems more feasible because of the lower values of Mach number and pressure occurring throughout the vacuum tube train system. The surface pressure variation plotted in Fig. 6g also shows the suitability of above mentioned elliptical model. The integrated pressure force can be observed to be minimum for this model.

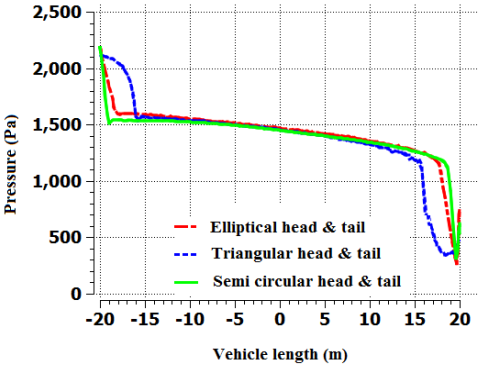

Fig. 6g - Pressure variation along the train for three different shapes of head and tail.

4. CONCLUSION

A computational study has been performed on the vacuum tube train system and various suitable parameters have been identified. The drag force acting in the system keeps varying and it needs to be at optimum levels. Through the simulations it was visible that the drag force increases with decreasing pressure and hence the pressure has to be maintained at a low value which is achievable and feasible in terms of cost and construction. The fastest velocity with which the train can travel with little shocks and vibrations has also been analysed and found to be 325 m/s, which corresponds to a Mach number of 0.936 which is in the transonic region, beyond which the system would turn into a supersonic region where the effects of shocks would be more severe. A comparison between three different train shapes has also been given and based on the values of drag force the suitable geometry has been arrived at, which is the elliptical train with a height to base ratio of 2:1.

REFERENCES

Bibin, S. and S. K. Mukherjea (2013). Numerical Investigation of Aerodynamic Drag on Vacuum Tube High Speed Train. In *ASME 2013 International Mechanical Engineering Congress and Exposition* (pp. V013T14A048-V013T14A048). American Society of Mechanical Engineers.

Chen, X., L. Zhao, J. Ma and Y. Liu (2012). Aerodynamic simulation of evacuated tube maglev trains with different streamlined designs. *Journal of Modern Transportation 20*(2), 115-120.

Kim, T. K., K. H. Kim and H. B. Kwon (2011). Aerodynamic characteristics of a tube train. *Journal of wind engineering and industrial aerodynamics 99*(12), 1187-1196.

Kwon, H. B., K. H. Jang, Y. S. Kim, K. J. Yee and D. H. Lee (2001). Nose shape optimization of high-speed train for minimization of tunnel sonic boom. *JSME International Journal Series C Mechanical Systems, Machine*

Elements and Manufacturing 44(3), 890-899.

Zhang, Y. (2012). Numerical simulation and analysis of aerodynamic drag on a subsonic train in evacuated tube transportation. *Journal of Modern Transportation 20*(1), 44-48.

Zhang, Y., D. Oster, M. Kumada, J. Yu and S. Li (2011). Key vacuum technology issues to be solved in evacuated tube transportation. *Journal of Modern Transportation 19*(2), 110-113.

Zhi-yun, S. H. E. N. (2005). On Developing High-Speed Evacuated Tube Transportation in China [J]. *Journal of Southwest Jiaotong University, 2, 000*.